

# CO<sub>2</sub> Fluxes to Aquifers Beneath Cropland: Merging Measurements and Modeling

Eike M. Thaysen<sup>1</sup>, Diederik Jacques<sup>2</sup>, and Eric Laloy<sup>2</sup>

<sup>1</sup>*Department of Chemical and Biochemical Engineering, Center for Ecosystems and Environmental Sustainability, Technical University of Denmark, Kgs. Lyngby, Denmark, [emth@kt.dtu.dk](mailto:emth@kt.dtu.dk)*

<sup>2</sup>*Institute for Environment, Health, and Safety, Belgian Nuclear Research Centre (SCK•CEN), Mol, Belgium, [djacques@sckcen.be](mailto:djacques@sckcen.be), [elaloy@sckcen.be](mailto:elaloy@sckcen.be)*

## Abstract

Carbon dioxide (CO<sub>2</sub>) fluxes in the vadose zone are influenced by a complex interplay of biological, chemical and physical factors. To determine the controls behind dissolved inorganic carbon (DIC) percolation to aquifers, CO<sub>2</sub> fluxes in planted soil mesocosms were described with the SOILCO<sub>2</sub> model formulation (Šimůnek et al., 1993) that was implemented into the HP1 module of the Hydrus 1D software package. Water flow, cation exchange, and supersaturation for amorphous aluminum hydroxide were modeled. The model provided a good fit to measured water content and outflow time series. Also, the measured DIC efflux, CO<sub>2</sub> partial pressure (pCO<sub>2</sub>), and CO<sub>2</sub> efflux were simulated well throughout most of the experimental period. However, alkalinity was significantly overestimated, indicating additional acidity production in the mesocosms. CO<sub>2</sub> fluxes were strongly influenced by a higher root growth in the mesocosms as compared to the field, which caused steep increases in pCO<sub>2</sub>. The model showed that the high pCO<sub>2</sub> triggered weathering of calcite, leading to increases in alkalinity. DIC percolation lacked accompanying increases, indicating an overestimation of the DIC percolation estimated from measured pCO<sub>2</sub>, alkalinity, and water flux.

## 1. Introduction

The global flux of carbon dioxide (CO<sub>2</sub>) into the groundwater is less than 1% of the diffusion flux of CO<sub>2</sub> from soils to the atmosphere (Kessler et al., 2001). Although estimates of leaching losses of carbon are scarce, available estimates indicate that leaching of dissolved carbon from soils constitutes a significant fraction of the annual carbon (C) budgets of croplands (Kindler et al., 2011). C is leached from soils as dissolved organic carbon (DOC), dissolved methane (CH<sub>4</sub>), and dissolved inorganic carbon (DIC). DIC originates from either soil respiration, dissolution of carbonate minerals, or atmospheric CO<sub>2</sub>. The latter contribution is negligible because of the low atmospheric partial pressures of CO<sub>2</sub> (pCO<sub>2</sub>) (Kindler et al., 2011). The amount of DIC varies with the soil pCO<sub>2</sub>, pH, and temperature (Clark et al., 1997). However, our understanding of production and transport of CO<sub>2</sub> in the soil (Jassal et al., 2005) and of the exchange of CO<sub>2</sub> between soils, plants, and the atmosphere is incomplete (Sugden et al., 2004).

In this work, experimentally determined CO<sub>2</sub> fluxes in the vadose zone of large planted soil mesocosms were modeled using the HP1 module of the Hydrus-1D software package (Jacques et al., 2010) in order to identify the main drivers controlling DIC transport to aquifers.

## 2. Methodology

### 2.1. Experimental Data

Soil from the A and C horizons of a carbonated alluvial sediment was collected and packed into plexiglas cylinders (length: 83 cm, diameter: 19 cm) above a bottom plate with an embedded suction disc (Thaysen et al., in review). The hydraulic connection between the C horizon and the suction disc was optimized by means of a thin layer of quartz flour and a layer of quartz flour mixed with the C horizon.

Barley (*Hordeum vulgare* L. cv Anakin) was sown into the mesocosms at a seeding density of 280 plants m<sup>-2</sup>. The mesocosms were incubated in climate chambers and maintained at mean daily air and night temperatures of 18 °C and 13 °C, respectively. Plants were irrigated with a 50% strength Hoagland solution (Hoagland et al., 1950) with an alkalinity of 0.05 meq L<sup>-1</sup>. Root length was measured at five time points on the outside of the mesocosm walls.

Volumetric water content (VWC) and temperature within the mesocosms were logged at ten minute intervals with 5 TM and EC-TM sensors and EM50 (Decagon Devices, USA) and CR1000 loggers (Campbell Scientific, UK). To increase measurement accuracy, sensors were calibrated to the A and C horizon conditions according to the guidelines of the manufacturers.

Samples of soil air and soil water were collected weekly and analyzed for CO<sub>2</sub> partial pressure (pCO<sub>2</sub>) and alkalinity, respectively. Soil air pCO<sub>2</sub> was measured on a 7890A GC System with a FID detector in combination with a methanizer (Agilent Technologies, DK). Alkalinity was determined using the Gran Titration method (Gran, 1952).

The exchange of CO<sub>2</sub> between the mesocosm and the atmosphere was measured at regular intervals using the static closed chamber technique (Ambus et al., 2007). During measurement, the concentration of CO<sub>2</sub> in the chamber space (V= 22.6 L) was continuously closed-loop sampled with an environmental gas monitor (EGM-2, PP-Systems, USA), and the flux was estimated from the concentration change, volume, and measurement time.

The DIC concentration in the percolating water was calculated from the pCO<sub>2</sub>, the alkalinity in the soil solution, and the temperature at the mesocosm bottom (~62-76 cm) using PHREEQC software (Parkhurst et al., 2011), while assuming chemical equilibrium between gaseous CO<sub>2</sub>, CO<sub>2(g)</sub>, and solution H<sub>2</sub>CO<sub>3</sub><sup>\*</sup>, HCO<sub>3</sub><sup>-</sup>, and CO<sub>3</sub><sup>2-</sup>. The DIC concentration was multiplied by the water flux to obtain the DIC flux to the groundwater.

### 2.2. Modeling of Experimental Results

Results from only one planted mesocosm are discussed in this paper. The mesocosm consisted of three materials. The first and second layers were the A and C horizons located between 0-30 and 31-80 cm depths, respectively. The suction plate, the quartz flour layer, and the layer of quartz flour mixed with the C horizon were grouped in the third material between depths of 80-83 cm.

### Model Setup

Water flow was described by the Richards equation and the constitutive relations of the van Genuchten-Mualem model without hysteresis (Mualem, 1978; van Genuchten, 1980). Upper boundary conditions for the water flow were atmospheric conditions with a surface boundary layer. At the bottom, a variable pressure head boundary condition was chosen. Maximum allowed pressure head at the soil surface was zero. Potential evapotranspiration was estimated using the Blaney Criddle formula (Blaney et al., 1962). Water retention parameters were obtained from inverse modeling of the water flow in an unplanted mesocosm (data not shown) using Hydrus-1D (Šimůnek et al., 2013) and a global stochastic optimization algorithm (Vrugt et al., 2009).

Heat transport was not included in the model as temperatures in the mesocosm were almost constant. Temperatures declined from the top to the bottom of the mesocosm due to the proximity of heat emitting lamps at the mesocosm top, high volumetric water content (VWC) in the A horizon and the higher heat capacity of water compared to air. Hence, constant boundaries of 22 and 18°C were used at the mesocosm top and bottom, respectively, with a linear interpolation in between. The model domain was discretized in 157 nodes with the highest node densities at the mesocosm top and at the interfaces of soil materials.

CO<sub>2</sub> production was modeled through implementation of equations and parameters for CO<sub>2</sub> production from SOILCO2 (Šimůnek et al., 1993; Suarez et al., 1993). The parameter  $a$ , describing the depth dependency of microbial respiration, was set to 0.04 cm<sup>-1</sup>, and the boundary layer height (BLH) was set at 0.05 m. The dependency of CO<sub>2</sub> production on root growth was accounted for by 1) a distribution factor and (measured) root depth (as is done for root water uptake) and 2) by introducing a linear root biomass increase,  $RMI [M]$ , (Eq. 2). The latter was added to account for a 2-5 times higher total root mass in mesocosms than in the field (Table 1) (Biscoe et al., 1975; Xu et al. 1992; Malhi 2002). It was anticipated that

$$RMI = R_{init} + r * time \quad (2)$$

where  $R_{init} [M]$  is the initial root mass at simulation time= 0 [T] and  $r$  is the growth rate [MT<sup>-1</sup>]. For our simulations  $R_{init}$  was set to 0.1 g and  $r$  was 0.21 g day<sup>-1</sup>.

Table 1. Root growth as a function of depth in mesocosms as measured 70 days after sowing.

Depth (cm)	Root mass (g) (means ± SE)	Root mass per soil horizon (%)	Total root mass (g m <sup>-2</sup> )
0-10	8.1 ± 0.5	91.7 ± 0.9	527.4 ± 14.7
10-20	3.5 ± 0.3		
20-30	2.6 ± 0.3		
30-42	0.5 ± 0.1	8.3 ± 0.9	
42-58	0.3 ± 0.1		
58-80	<0.01		

CO<sub>2</sub> transport in the gas and water phases and phase distribution were described as stated within HP1. For more details the reader is referred to Šimůnek et al. (2013). The measured pore water composition was supersaturated for amorphous aluminum hydroxide, Al(OH)<sub>3(a)</sub>. Therefore, the saturation index (SI) of Al(OH)<sub>3(a)</sub> was set at 0.8 and 0.6 for the A and C horizons, respectively. The cation exchange capacity was estimated from the soil organic matter and clay content, resulting in values of 9.2\*10<sup>-2</sup> and 4.2\*10<sup>-3</sup> eq dm<sup>-3</sup> for the A and C horizons, respectively. The exchanger composition was calculated from the soil water composition on day 40 and contained 3.90\*10<sup>-2</sup> Ca<sup>2+</sup>, 6.51\*10<sup>-3</sup> Mg<sup>2+</sup>, 6.62\*10<sup>-4</sup> K<sup>+</sup>, 1.39\*10<sup>-4</sup> Na<sup>+</sup>, 1.32\*10<sup>-4</sup> Al(OH)<sub>2</sub><sup>-</sup> and 4.04\*10<sup>-5</sup> Al<sup>3+</sup> mol dm<sup>-3</sup> in the A horizon, and 1.7\*10<sup>-3</sup> Ca<sup>2+</sup>, 2.863\*10<sup>-3</sup> Mg<sup>2+</sup>, 1.06\*10<sup>-4</sup> K<sup>+</sup>, 1.52\*10<sup>-4</sup> Na<sup>+</sup>, 2.4\*10<sup>-5</sup> Al(OH)<sub>2</sub><sup>-</sup> and 1.41\*10<sup>-5</sup> Al<sup>3+</sup> mol dm<sup>-3</sup> in the C horizon. To simplify the simulations, the influence of nutrients in the irrigation water was neglected.

### 3. Results and Discussion

#### 3.1. Water Flow

Water flow throughout the soil profile was generally well described (forward simulation from fitted parameters in an unplanted mesocosm, Fig. 1). However, due to a pressure drop across the suction disc that offset boundary conditions and the lack of retention parameters for material three, outflow and VWC in the soil profile could not be matched with high accuracy at the same time. Water logging at the mesocosm bottom (76 cm) was overestimated but cumulative outflow was simulated correctly.

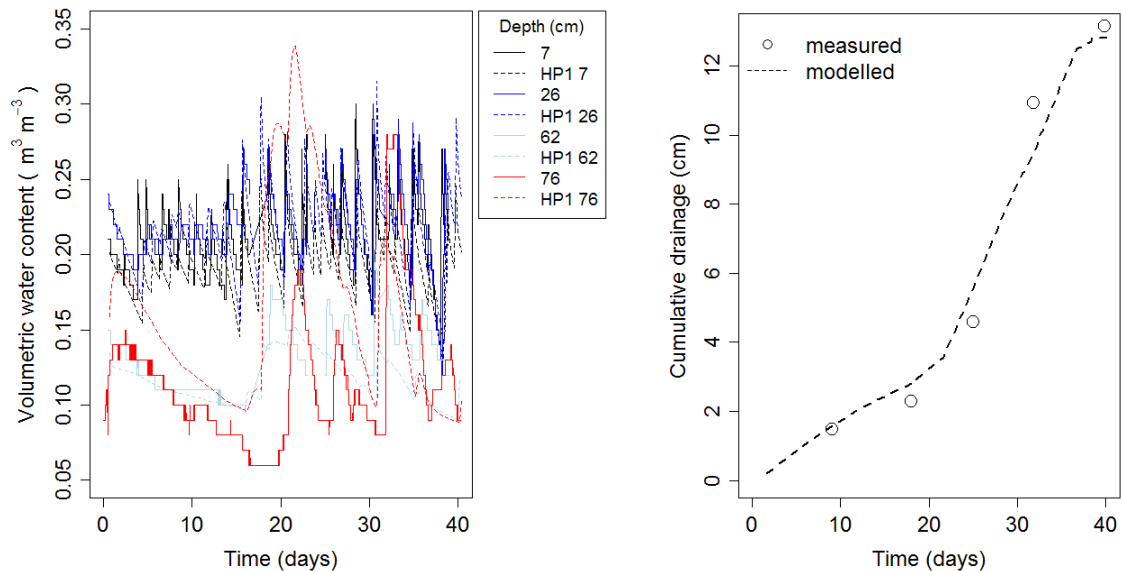


Figure 1. Measured and modeled water content profile and cumulative drainage.

### 3.2. Profiles of CO<sub>2</sub> and Alkalinity

The pCO<sub>2</sub> increased with plant growth. The magnitude of the pCO<sub>2</sub> could be simulated but the model could not capture all fluctuations in pCO<sub>2</sub> (Fig. 2). The diffusion gradient was matched quite well on days 7, 21 and 35. However, the measured gradients on days 27 and 40 were significantly steeper than the simulated ones. The addition of dependency of CO<sub>2</sub> production on the root biomass increase caused a steady increase in pCO<sub>2</sub> with root growth. On the other hand, the distribution of the production within the soil profile is defined by the normalized root distribution. However, the current implementation of the evolution of the normalized root distribution in HYDRUS simulates a downward shift of the center of mass of the roots (Šimůnek et al., 2013). This downward shift of the region of the highest root abundance seems to be an erroneous assumption for a mesocosm in which ~90% of the root biomass is found in the upper 30 cm after harvest, and root growth declines exponentially from the top (Table 1). Root mass always declines with soil depth (Malhi et al., 2002) and exponential decreases have often been reported (e.g., Xu et al., 1992; Mandal et al. 2003; Rong-hua et al., 2008).

The observed peak pCO<sub>2</sub> in mesocosms was 2-5% higher than observed at a corresponding field site (Voulund, Denmark, 56°2'35.7"N, 9°8'101.1"E). Peak pCO<sub>2</sub> levels were also 5-7% higher than in a previous field study addressing CO<sub>2</sub> dynamics under actively growing winter wheat in a silt loam soil at similar soil temperatures and VWC (Buyanovsky et al., 1983). The higher pCO<sub>2</sub> in mesocosms is probably caused by the higher root length in mesocosms as compared to the field.

The alkalinity increased throughout the experimental period (Fig. 2). Increases in alkalinity could be modeled, but simulated values were twice the measured values. Increases in alkalinity can be understood from 1) increased dissolution of CO<sub>2(g)</sub> into soil water as the pCO<sub>2</sub> in mesocosms increases (Eq. 2) and 2) the consumption of carbonic acid, H<sub>2</sub>CO<sub>3</sub>, during dissolution of calcite, CaCO<sub>3</sub>, that causes 3) increases in [HCO<sub>3</sub><sup>-</sup>] (Eq. 3).

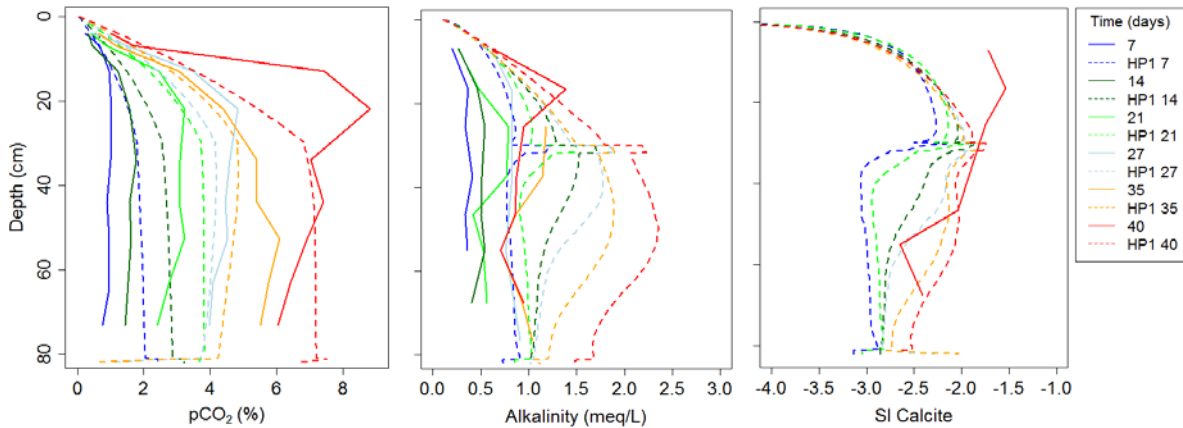
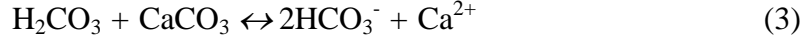


Figure 2. Measured and modeled time course of soil air pCO<sub>2</sub>, alkalinity, and saturation index (SI) for calcite.



Calcite dissolution on day 40 (Fig. 2) could be approximated by the model in the C horizon but was underestimated in the A horizon, which can be ascribed to the underestimation of  $\text{pCO}_2$  on day 40. The larger increases in alkalinity in the simulation as compared to the measured values indicate additional alkalinity-consuming acid production in the mesocosm that is not covered by the model. This could be organic acids released by the roots although several authors have suggested that organic acid concentrations in nutrient-rich bulk soil are generally low (Drever et al., 1994; Ryan et al., 2001) to non-detectable (Baars et al., 2008). Alternatively, watering with a nutrient solution low in alkalinity might also have decreased the soil alkalinity due to the combined effects of flushing and cation exchange with sediment-bound base cations. It is also possible that modeling of proton exchange, which has been shown to act as a source of acid in  $\text{NaHCO}_3$  water in which calcite dissolves (Appelo, 1994), could produce the measured profiles of alkalinity. The incorporation of additional acid-producing processes in future model work is planned and is expected to improve model fits to experimental data.

### 3.3. $\text{CO}_2$ Fluxes out of the Mesocosm

The simulated ecosystem respiration (ER) was slightly lower than the measured ER at days 0-30 (Fig. 3) although the diffusion gradients for  $\text{pCO}_2$  were simulated well on days 7-21 and 35 (Fig. 2). Simulated ER was much lower than measured ER on days 30-40 (Fig. 3). This is due to the underestimation of the  $\text{pCO}_2$  in the A horizon towards the end of the experiment as discussed in Section 3.2. Due to the much higher  $\text{pCO}_2$  in mesocosms, measured ER was larger than what has been reported in the field under similar environmental conditions (Buyanovksy et al., 1986; Buyanovsky et al., 1983; Feizene et al., 2008). The simulated  $\text{CO}_2$  efflux follows the applied irrigation pattern with lower efflux during irrigation events.

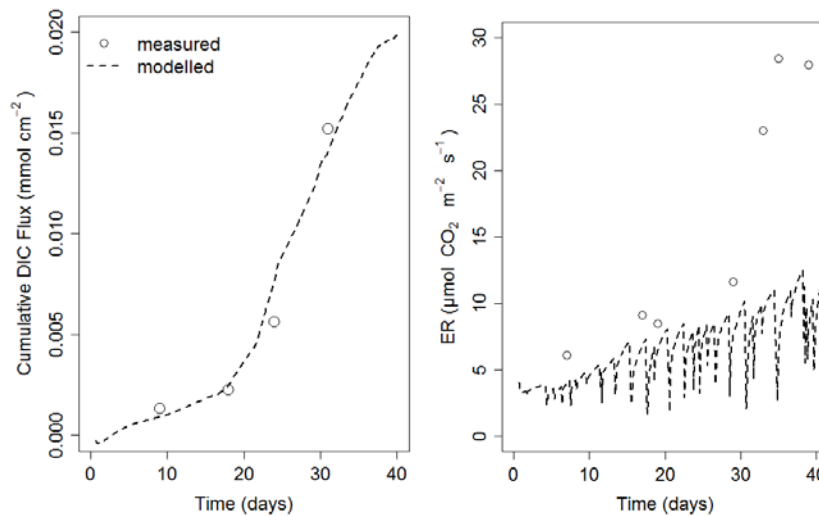


Figure 3. Measured and modeled time course of ecosystem respiration (ER) and DIC percolation.

DIC percolation was predicted well although alkalinity was largely overestimated (Fig. 3). According to theory (Appelo et al., 2005), the DIC concentration can be calculated from  $\text{pCO}_2$

and soil alkalinity. DIC percolation is then described by the product of the [DIC] and the drainage flux (e.g., Kindler et al., 2011; Walmsley et al., 2011). As the drainage from the mesocosm was simulated well (Fig. 1), the large overestimation of alkalinity was expected to increase DIC percolation compared to the measured. While differences between the measured and simulated DIC percolation might be due to the fact that the measured DIC percolation was estimated from a weekly “snap shot” of the pCO<sub>2</sub> and the alkalinity, as has been suggested by Walmsley et al. (2011), these inconsistencies need further investigation. The average [DIC] of  $2.5 \pm 0.02 \text{ mmol L}^{-1}$  was in the range of previously reported values for cropped carbonated soil: Luvisol with sand-loam texture ([DIC]:  $1.90 \text{ mmol L}^{-1}$ ) (Siemens et al., 2012) and calcareic Cambisol with silt-loam texture ([DIC]:  $5.9 \text{ mmol L}^{-1}$ ) (Kindler et al., 2011).

#### 4. Conclusion

CO<sub>2</sub> fluxes in the vadose zone of planted mesocosms were strongly influenced by root growth that caused steep increases in CO<sub>2</sub>, triggering the dissolution of calcite with subsequent increases of alkalinity. The applied simple model was able to simulate the main tendencies in the data and aided in the comprehension of the underlying biogeochemical processes. The model stressed that additional acid-producing processes occurred in the mesocosm that were not detectable from experimental results alone. Incorporation of the latter in future model work is planned and is expected to improve model fits to experimental data. Modeling results further indicated that pCO<sub>2</sub> profiles are strongly linked to the root distribution and that the downward shift of the center root mass with plant age (root growth) would need to be revised to improve the model.

#### Acknowledgements

The authors thank Rasmus Jakobsen, Søren Jessen, and Jirka Šimůnek for their support and discussion.

#### References

- Ambus, P., S. O. Petersen, and J. F. Soussana, Short-term carbon and nitrogen cycling in urine patches assessed by combined carbon-13 and nitrogen-15 labelling, *Agr. Ecosyst. Environ.*, *121*, 84-92, 2005
- Appelo, C. A. J., Cation and proton exchange, pH variations, and carbonate reactions in a freshening aquifer, *Water Resour. Res.*, *30*, 2793-2805, 1994.
- Appelo, C. A. J., and D. Postma, *Geochemistry, Groundwater and Pollution*, 2nd edition Edition. Balkema, 2005.
- Baars, C., T. H. Jones, and D. Edwards, Microcosm studies of the role of land plants in elevating soil carbon dioxide and chemical weathering, *Global Biogeochem.*, *22*, 1-9, 2008.
- Biscoe, P. V., R. K. Scott, and J. L. Monteith, Barley and its environment. III. Carbon budget of the stand, *J. Appl. Ecol.*, *12*, 269-290, 1975.
- Blaney, H. F., and W. D. Criddle, Determining consumptive use and irrigation water requirements, In: “*USDA Technical Bulletin*”, Beltsville, US Department of Agriculture, 1962.
- Buyanovksy, G. A., G. H. Wagner, and C. J. Gantzer, Soil respiration in a winter wheat ecosystem, *Soil Sci. Soc. Am. J.*, *50*, 338-344, 1986.
- Buyanovsky, G. A., and G. H. Wagner, Annual cycles of carbon dioxide level in soil air, *Soil Sci. Soc. Am. J.*, *47*, 1139-1145, 1983.

- Drever, J. I., and G. F. Vance, *Role of Soil Organic Acids in Mineral Weathering Processes, Organic Acids in Geological Processes* (Eds. Pittman, E.D., and MD. Lewan), Springer, Berlin, 138-161, 1994.
- Feizene, D., V. Povilaitis, and G. Kadziene, Springtime soil surface respiration and soil vapour flux in different long-term agro-ecosystems, *Ekologija*, 54, 216-225, 2008.
- Gran, G., Determination of the equivalence point in potentiometric titrations 2, *Analyst*, 77, 661-671, 1952.
- Hoagland, D. R., and D. I. Amon, The water-culture method for growing plants without soil, Circ. 347. Univ. of Calif. Agric. Exp. Station, Berkley., Vol C347 rev 1950. College of Agriculture, University of California, Berkeley, 1950.
- Jacques, D., and J. Šimůnek, Notes on HP1 – a software package for simulating variably-saturated water flow, heat transport, solute transport and biogeochemistry in porous media, *SCK•CEN-BLG-1068*, 2010.
- Kessler, T. J., and C. F. Harvey, The global flux of carbon dioxide into groundwater, *Geophys. Res. Lett.*, 28, 279-282, 2001.
- Kindler, R., J. Siemens, K. Kaiser, D. C. Walmsley, C. Bernhofer, N., Buchmann, P. Cellier, W. Eugster, G. Gleixner, T. Grünwalds, A. Heim, A. Ibrom, S. Jones, M. Jones, S. Lehuger, B. Loubet, R. McKenzie, E. Moors, B. Osborne, K. Pilegaard, C. Rebmann, M. Saunders, M. W. I. Schmidt, M. Schrupf, J., Seyferth, U. Skiba, J.-F. Soussana, M. A. Sutton, C. Tefs, B. Vowinkel, M. J. Zeeman, and M. Kaupenjohann, Dissolved carbon leaching from soil is a crucial component of the net ecosystem carbon balance, *Global Change Biol.*, 17, 1167–1185, 2011.
- Malhi, S. S. and K. S. Gill, Fertilizer N and P effects on root mass of bromegrass, alfalfa and barley, *Journal of Sustainable Agriculture*, 19(3), 51-63, 2002.
- Mandal, K. G., K. M. Hati, A. K. Misra, P. K. Ghosh, and K. K. Bandyopadhyay, Root density and water use efficiency of wheat as affected by irrigation and nutrient management, *Jour. Agric. Physics*, 3(1), 49-55, 2003.
- Mualem, Y., Hydraulic conductivity of unsaturated porous media: Generalized macroscopic approach, *Water Resour. Res.*, 14, 325–334, 1978.
- Parkhurst, D., and C. A. J. Appelo, PHREEQC (Version 3)--A Computer Program for Speciation, Batch-Reaction, One-Dimensional Transport, and Inverse Geochemical Calculations (Denver, Colorado, USA, U.S. Geological Survey, Water Resources Division), 2013.
- Rong-hua, L., Z. Zi-Xi, F. Wen-Song, D. Tian-Houg, and Z. Guo-Giang, Distribution pattern of winter wheat root system, *Shengtaixue Zazhi*, 27(11), 2024-2027, 2008.
- Ryan, P. R., E. Delhaize, and D. L. Jones, Function and mechanism of organic anion exudation from plant roots, *Annu Rev Plant Physiol Plant Mol Biol.*, 52, 527-560, 2001.
- Siemens, J., A. Pacholski, K. Heiduk, A. Giesemann, U. Schulte, R. Dechow, M. Kaupenjohann, and H.-J. Weigel, Elevated air carbon dioxide concentrations increase dissolved carbon leaching from a cropland soil, *Biogeochemistry*, 108, 135-148, 2012.
- Šimůnek, J., M. Šejna, H. Saito, M. Sakai, and M.Th. van Genuchten, The Hydrus-1D Software Package for Simulating the Movement of Water, Heat, and Multiple Solutes in Variably Saturated Media, Version 4.16, *HYDRUS Software Series 3* (Riverside, California, USA, Department of Environmental Sciences, University of California Riverside), 2013.
- Šimůnek, J., and D. L. Suarez, Modeling of carbon dioxide transport and production in soil. 1. Model development, *Water Resour. Res.*, 29, 487-497, 1993.
- Suarez, D. L., and J. Šimůnek, Modeling of carbon dioxide transport and production in soil. 2. Parameter selection, sensitivity analysis, and comparison of model predictions to field data, *Water Resour. Res.*, 29, 499-513, 1993.
- Sugden, A., R. Stone, and C. Ash, Ecology in the underworld – Introduction, *Science*, 304, 1613-1613, 2004.
- Thaysen, E. M., S. Jessen, P. Ambus, C. Beier, D. Postma, and I. Jakobsen, Technical Note: Mesocosm approach to carbon dioxide fluxes across the vadose zone in croplands, submitted to *Biogeosciences*.

- van Genuchten, M. Th., A closed-form equation for predicting the hydraulic conductivity of unsaturated soils, *Soil Sci. Soc. Am. J.*, 44, 892-898, 1980.
- Vrugt, J. A., B. A. Robinson, and J. M. Hyman, Self-adaptive multimethod search for global optimization in real-parameter spaces, *IEEE Transactions on Evolutionary Computation*, 13, 243-259, 2009.
- Walmsley, D. C., J. Siemens, R. Kindler, L. Kirwan, K. Kaiser, M. Saunders, M. Kaupenjohann, and B. A. Osborne, Dissolved carbon leaching from an Irish cropland soil is increased by reduced tillage and cover cropping, *Agr. Ecosyst. Environ.*, 142, 393-402, 2011.
- Xu, J. G., and N. G. Juma, Above- and below-ground net primary production of four barley (*Hordeum vulgare* L.) cultivars in western Canada, *Can. J. Plant. Sci.*, 72, 1131-1140, 1992.

